Catalytic Transformation of C_7-C_9 Methyl Benzenes over USY-based FCC Zeolite Catalyst

S. Al-Khattaf*, N. M. Tukur, A. Al-Amer and U. A. Al-Mubaiyedh

Chemical Engineering Department, King Fahd University of Petroleum & Minerals
Dhahran 31261, Saudi Arabia

Abstract

Catalytic transformation of three methyl benzenes (*toluene, m-xylene, and 1,2,4-trimethyl benzene*) has been investigated over USY based FCC zeolite catalyst in a novel riser simulator at different operating conditions. The effect of reaction conditions on the variation of isomerization to disproportionation products ratio (I/D), distribution of trimethylbenzene (TMB) isomers (1,3,5-to-1,2,3-) and values of *p*-xylene/*o*-xylene (P/O) ratios are reported. The sequence of reactivity of the three alkyl benzenes was found to decrease as the number of methyl group per benzene ring decreases, as follows: *1,2,4-trimethyl benzene* > *m-xylene* > *toluene.* This is true at all temperatures investigated over the USY zeolite. Toluene was found unreactive in our reaction condition. Effectiveness factor (η_{ss}) of both1,2,4-TMB and *m*-xylene have been estimated. While *m*-xylene's η_{ss} was close to unity at all condition, 1,2,4-TMB's η_{ss} was less than that of *m*-xylene. The effectiveness factor was estimated from the quasi-steady state approximation modeling of the experimental data involving a decay function based on "Time on Stream". Based on the present study, it was found that the number of methyl groups has the most important role on the reactivity of 1,2,4-TMB, *m*-xylene and Toluene over Y-based catalyst.

December 2005

Keywords: FCC zeolite catalyst; USY; Toluene; *m*-Xylene; Disproportionation; Isomerization

*Corresponding author. Tel.: +966-3-860-1429; Fax: +966-3- 860-4234
e-mail address: skhattaf@kfupm.edu.sa

1. Introduction

The demand for xylenes as a raw material for polyester fibers and films continues to grow and drive the search to increase xylene production processes. In the year 1999, the world consumption of mixed xylene was about 24 million tons, and is expected to grow at a rate of 6.2% to 32.5 million tons by the year 2004. This indicates that xylenes are still gaining importance in the petrochemical market. Most of the currently working isomerization plants are using zeolite based catalysts.

One common way for xylene production is the conversion of the lower value toluene (C_7) and trimethylbenzene (C_9) into xylenes. Considerable research effort has been devoted for this purpose. It is well known that these hydrocarbons undergo several simultaneous chemical reactions which include; Isomerization, disproportionation, transalkylation, dealkylation, and coke formation.

Toluene transformation to other aromatics is well documented in the literature [1,2,3]. This transformation can take place through two major different techniques. The first is toluene hydrodealkylation where toluene is converted to benzene in the presence of hydrogen. The other technique is disproportionation where two toluene molecules react together to form benzene and xylene. Mobil disproportionation process (TDP-3^{SM}) is among the most famous commercial processes for toluene disproportionation [4]. Most of the reported studies on toluene disproportionation have been conducted at relatively high pressure and in the presence of hydrogen using fixed bed reactor. The equilibrium mixture contains approximately 24% *p*-xylene, 54% *m*-xylene and 22% *o*-xylene in the temperature range of 250-450^{o}C. ZSM-5 zeolites can be used in toluene disproportionation to enhance *para*-selectivity higher than 90% [5].

Detailed mechanism of toluene disproportionation was reported by Xiong et al.[1]. Two different reaction pathways were proposed, i.e., methyl transfer mechanism (formation of a methoxy group on the zeolite surface) and the diphenyl methane mechanism. It was shown that toluene disproportionation does not require Brönsted acid sites of a high acid strength (present in H-ZSM-5 zeolite) to proceed, and the rate of the reaction is controlled by the concentration of acid sites, which is higher in zeolite Y compared to H-ZSM-5 [1]. Olson and Haag [6] indicated that for para-selective toluene disproportionation, the primary toluene disproportionation to xylenes, and the subsequent xylene isomerization to *p*-xylene should be controlled to achieve higher than equilibrium concentration of *p*-xylene by

ensuring that the reaction is not diffusion limited and the diffusivity of *p*-xylene in the zeolite channel is higher compared to *o*- and *m*-xylene. This is to ensure that para-isomer is removed much faster from the channel system than the other isomers [7].

m-xylene isomerizes to the *para* and *ortho* isomers and can disproportionate into trimethylbenzenes (TMBs) and toluene. It has been proposed by Morin et al., [8] and Morin et al., [9] that disproportionation can take place through the formation of benzylic carbocations and trimethyl diphenylmethanes intermediates. On the other hand, two different mechanisms have reported for *m*-xylene isomerization. Monomolecular pathway which involves the formation benzenium ion intermediate and bimolecular pathway involving disproportionation reaction between two xylene molecules forming trimethylbenzene and toluene. Transalkylation reaction subsequently occurs between trimethylbenzene and *m*-xylene. Evidence of the presence of a bimolecular pathway in the isomerization of xylene on some large-pore zeolites has been reported by Corma and Sastre [10,11]. It has been reported by Morin et al., [8] and Morin et al., [9] that bimolecular isomerization is more selective to *o*-xylene than to *p*-xylene.

Catalytic data of *m*-xylene transformation over acid catalysts provides insights into catalyst structure and pore-size [12]. A larger value of the *para/ortho* (P/O) ratio of the products corresponds to smaller catalyst pore size and vice versa. The distribution of trimethylbenzenes gives useful information about the pore structure of zeolites [13]. In zeolites with 12 MR, Martens et al. [14] showed that zeolites with adjacent cages favor the formation of the bulky 1,3,5-trimethylbenzene isomer while zeolites with straight channels and side pockets at regular distances, such as mordenite (MOR), are favorable for the formation of the 1,2,3-trimethylbenzene isomer. The ratio of the rates of isomerization to disproportionation (I/D), similar to the P/O ratio, is useful in providing information about the pore or cage size. Since disproportionation necessarily requires a bimolecular reaction, larger pore systems that can accommodate the required transition state give more disproportionation. In addition, the *m*-xylene reactions can also provide a means of determining rates of deactivation via carbon depositing mechanisms [15].

Ilyas and Al-Khattaf [16] have carried out a systematic study on the influence of reaction conditions (temperature, time, and reactant type) on the selectivity of xylene transformation over USY zeolite. Initial product selectivity revealed that both isomerization and disproportionation of xylenes are primary reactions. Higher conversion was observed with *p*-xylene reactant as compared to *m*- and *o*-xylene. Furthermore, a comprehensive

kinetic model for xylenes isomerization and disproportionation has been reported by Ilyas and Al-Khattaf [17] and Al-Khattaf et al., [18]. This kinetic modeling is based on the triangular reaction scheme and time on stream deactivation function. All activation energies for different reaction steps have been evaluated and compared with literature and has been found that *m*-xylene disproportionation activation energy is higher than that of isomerization.

Trimethyl benzene transformations have been investigated over medium-pore zeolites like ZSM-5 and large-pore zeolites such as Y, Beta, and also mordenite. Collins et al. [19] investigated the transformation (isomerization and disproportionation) of trimethylbenzenes (TMBs) over LaY catalysts. In the disproportionation reaction, the transfer of one methyl group from TMBs led to the formation of equal amount of xylene and tetramethylbenzene (TeMBs) isomers. Authors reported that disproportionation appeared to be linearly related to the total conversion over most of the conversion range studied for both 1,2,4- and 1,3,5-TMB, whereas for 1,2,3-TMB, isomerization was much more favored than disproportionation. They also observed that the pre-dried LaY catalyst was 2 to 3 times more active for disproportionation than the other catalyst calcined by rapid heating of the wet cake. The work by Matsuda et al., [20] concluded that isomerization reaction can take place only over Bronsted acid sites, whereas both Bronsted and Lewis sites are responsible for disproportionation reaction.

Roger et al. [21,22] studied the conversion of 1,2,4- Trimethylbenzene (1,2,4-TMB) over amorphous silica-alumina and HZSM5 in the gas phase and investigated the effect of pore mouth narrowing. They concluded that paring reaction played a decisive role during the conversion over HZSM5 at elevated temperature (450^{o}C) and in the reaction sequence, xylenes and tetramethylbenzenes (TeMBs) were intermediates. Over both silica-alumina and HZSM5, isomerization of 1,2,4-TMB to 1,2,3- and 1,3,5-TMB isomers were found to be the most rapid reaction with about 90% selectivity at low conversion and this 1,2-methyl-shift were shown to take place on the external surface of the zeolite crystals. They also reported that over silica-alumina, the reaction almost terminated at the disproportionation step, whereas over HZSM5, the disproportionation of 1,2,4-TMB was followed by rapid paring dealkylation of the TeMBs. The bulky intermediates (TeMBs) that reinforced the diffusional resistances by pore mouth narrowing favored the paring reaction inside the zeolite crystals.

Recently, Atias et al. [23] developed a heterogeneous kinetic model for the catalytic conversion of 1,2,4-trimethylbenzene in a CREC riser using USY zeolite catalysts under FCC operating conditions. They determined the intrinsic kinetic parameters for both isomerization and disproportionation reactions. Cejka et al. [24] studied the effect of the structure of large pore zeolites on the activity, selectivity and time-on-stream (T-O-S) in trimethyl benzene disproportionation. They used zeolites of beta, Y, L and Mordenite types which exhibited significant difference in conversion and T-O-S. They found higher conversions of TMBs and high selectivity to xylenes and TMBs at 400^{o}C with zeolites Y and beta (which provides optimum reaction space) compared to other large pore sieves (Mordenite and zeolites L). They also measured the diffusion coefficients of 1,2,4- and 1,3,5-TMBs and 1,2,3,5-TeMBs at 25 and 100^{o}C over zeolites Y, beta and Mordenite and the measured values followed the decreasing order of *m*-xylene >> 1,2,4-TMB > 1,3,5-TMB ≈ TeMB.

Although abundant literature has been published on methyl benzenes transformation, however, most studies have focused on the effect of catalyst structure on the transformation of certain methyl benzene molecule. A comparison between the reactivity of different methyl benzene molecules having different number of methyl group along with their diffusion characteristics is still needed. Thus, the present study is aimed at investigating methyl benzenes transformation (toluene, *m*-xylene, and 1,2,4-trimethyl benzene) over USY-based FCC zeolite catalyst (FCC-Y) in a fluidized-bed reactor. The study will focus on the effect of catalyst structure and reaction conditions (time, temperature, and conversion) on the variation of the ratios of disproportionation to isomerization products (D/I), distribution of trimethylbenzene (TMB) isomers (1,3,5-to-1,2,3-) and values of *p*-xylene/*o*-xylene (P/O) ratios. The effectiveness factor for both *m*-xylene and 1,2,4-TMB will be estimated.

2. Experimental Procedure

2.1 The Riser Simulator

All the experimental runs were carried out in the Riser Simulator. This reactor is a novel bench scale equipment with internal recycle unit invented by de Lasa [25] to overcome the technical problems of the standard micro-activity test (MAT), and it is fast becoming a valuable experimental tool for reaction evaluation involving model compounds

[26,27], and also for testing and developing new FCC in VGO cracking [28,29]. The Riser Simulator consists of two outer shells, the lower section and the upper section which allow to load or to unload the catalyst easily. The reactor was designed in such way that an annular space is created between the outer portion of the basket and the inner part of the reactor shell. A metallic gasket seals the two chambers with an impeller located in the upper section. A packing gland assembly and a cooling jacket surrounding the shaft provide support for the impeller. Upon rotation of the shaft, gas is forced outward from the center of the impeller towards the walls. This creates a lower pressure in the centre region of the impeller thus inducing flow of gas upward through the catalyst chamber from the bottom of the reactor annular region where the pressure is slightly higher. The impeller provides a fluidized bed of catalyst particles as well as intense gas mixing inside the reactor. A schematic diagram of the Riser Simulator is shown in **Fig. 1**. A detailed description of various Riser Simulator components, sequence of injection and sampling can be found in Kraemer [30].

2.2 Materials

Ultrastable Y zeolite (USY) was obtained from Tosoh Company. The Na-zeolite was ion exchanged with NH_4NO_3 to replace the sodium cation with NH_4^+. Following this, NH_3 was removed and the H form of the zeolite was spray-dried using kaolin as the filler and silica sol as the binder. The resulting 60-μm catalyst particles had the following composition: 30 wt% zeolite, 50 wt% kaolin, and 20 wt% silica sol. The process of sodium removal was repeated for the pelletized catalyst. Following this, the catalyst was calcined for 2 hr at 600^{o}C. Finally, the fluidizable catalyst particles (60-μm average size) were treated with 100% steam at 760^{o}C for 5 hr.

Analytical grade (99% purity) pure toluene, *m*-xylene, and 1,2,4-trimethylbenzene were obtained from Sigma-Aldrich. All chemicals were used as received as no attempt was made to further purify the samples.

2.3 Procedure

Regarding the experimental procedure in the Riser Simulator, 0.8g of catalyst was weighed and loaded into the Riser Simulator basket. The system was then sealed and tested for any pressure leaks by monitoring the pressure changes in the system. Furthermore, the reactor was heated to the desired reaction temperature. The vacuum box was also heated to around 250^{o}C and evacuated at around 0.5psi to prevent any condensation of hydrocarbons

inside the box. The heating of the Riser Simulator was conducted under continuous flow of inert gases (argon) and the process usually takes few hours until thermal equilibrium is finally attained. Meanwhile, before the initial experimental run, the catalyst was activated for 15 minutes at 620^{o}C in a stream of air. The temperature controller was set to the desired reaction temperature, in the same manner the timer was adjusted to the desired reaction time. At this point the GC is started and set to the desired conditions.

Once the reactor and the gas chromatograph have reached the desired operating conditions, the feed stock was injected directly into the reactor via a loaded syringe. After the reaction, the four port valve immediately opens ensuring that the reaction was terminated and the entire product stream sent on-line to the analytical equipment via a pre-heated vacuum box chamber.

2.4 Analysis

The riser simulator operates in conjunction with a series of sampling valves that allow, following a predetermined sequence, one to inject reactants and withdraw products in short periods of time. The products were analyzed in an Agilent 6890N gas chromatograph with a flame ionization detector and a capillary column INNOWAX, 60-m cross-linked methyl silicone with an internal diameter of 0.32 mm.

Experiments were carried out at catalyst/reactant ratio of 5 (weight of catalyst = 0.81g, weight of reactant injected = 0.162g); residence times of 3, 5, 7, 10, 13 and 15 s; and temperatures of 400, 450 and 500^{o}C. During the course of the investigation, a number of runs were repeated to check for reproducibility in the conversion results, which was found to be excellent. Typical errors were in the range of ± 2%.

3. Kinetic Model Development

The riser simulator being a constant volume batch reactor unit, operated isothermally, a suitable material balance equation that describes reactant disappearance is given by Al-Khattaf and de Lasa [27] as:

$$-\frac{V}{W_{cr}}\frac{dC_A}{dt} = \eta_{ss} r_A \qquad (1)$$

where C_A is the reactant concentration in the riser simulator; V the volume of the reacting mixture; W_{cr} the mass of the catalysts in the reacting system; η_{ss} an effectiveness factor to

account for the influence of the pore diffusion resistance on the overall reaction rate; and r_A the reaction rate.

Considering that FCC cracking of model compounds follows a first order model, eq 1 can be expressed as:

$$-\frac{V}{W_{cr}}\frac{dy_A}{dt} = \eta_{ss} k_{A,in} \varphi_{in} y_A \tag{2}$$

Where y_A is the mass fraction of species A, $k_{A,in}$ is the intrinsic kinetic parameter, and φ_{in} is the intrinsic decay function that takes into account the deactivation of the catalyst.

A classical approach while describing catalyst decay is to consider catalyst decay as function of time-on-stream. A classical relationship is the one proposed by Voorhies [31]:

$$\varphi = \exp(-\alpha t) \tag{3}$$

where α is a constant and t is the time the catalyst is exposed to a reactant atmosphere (time–on-stream [TOS]). Considering that $k_{A,in}$ can be redefined as $k_{A,in} = k_0^{'} \times \exp\left[-E_R / R\left(1/T - 1/T_0\right)\right]$, eq 2 can be rewritten as follows:

$$-\frac{V}{W_{cr}}\frac{dy_A}{dt} = \eta_{ss} k_0^{'} \exp\left[\frac{-E_R}{R}\left(\frac{1}{T} - \frac{1}{T_0}\right)\right] \exp(-\alpha t)\, y_A \tag{4}$$

The effectiveness factor (η_{ss}) expresses the extent of diffusional constraints inside a catalyst. For a zeolite crystal under steady state, η_{ss} is defined as the ratio of the actual reaction rate to the reaction rate in the absence of internal diffusional resistance.

$$\eta_{ss} \approx \frac{\tanh\left(h^{'}\right)}{h^{'}} \tag{5}$$

Where $h^{'}$ is the modified Thiele Modulus, defined as;

$$h^{'} = \frac{1}{a_{ext}} \sqrt{\frac{k_{A,in} \rho_{cr} \varphi_{in}}{D_{eff}}} \tag{6}$$

with a_{ext} being the specific external surface area for the zeolite crystal (a_{ext}=6/D_{cr}), D_{eff} the effective diffusivity, and ρ_{cr} is the zeolite density (825 kg/m^3). The effective diffusivity coefficient in zeolites can be represented as:

$$D_{eff} = D_0 \exp\left(-\frac{E_D}{RT}\right) \tag{7}$$

where E_D represents the diffusion activation energy.

Eq 7 is very useful in estimating temperature effect on reactant transport. Based on the experimental results reported by Germanus et al.[32] for *m*-xylene diffusivity over NaX crystals in the temperature range of about 400K, energy of activation of 5.0-6.0 kcal/mol and D_O = 5 x 10^{-7} cm^2/s were estimated by the authors. In a recent work, Cejka et al., [24] reported the value of *m*-xylene diffusion coefficient to be at least one order higher than those of trimethyl benzenes. Thus, [E_D=6 kcal/mol and D_O = 5 x 10^{-8} cm^2/s] will be used as estimate for the diffusivity of 1,2,4-TMB. Thus, the above reported E_D and D_O values will be employed in calculation of the effectiveness factor (η_{ss}) for both molecules.

Therefore, catalytic conversion of the methyl benzenes in the riser simulator can be modeled using a set of two equations, namely, eqs 4 and 5. Since the diffusion parameters (D_O and E_D) are known, only three intrinsic kinetic parameters ($k_0^{'}$, E_R, and α) need to be determined to fully characterize the diffusive- reactive system.

4. Results and Discussions

4.1 Catalyst Characterization

Zeolite catalysts for use in fluidized-bed reactors are often incorporated in amorphous matrix to achieve the desired fluidization of the catalyst particles. As a result, the determination of the crystallinity and phase purity of the zeolite samples in the presence of this matrix is important in catalytic reactions. The results of the catalyst characterization are presented in **Table 1**. The total acidity was determined by NH_3 adsorption (TPD) and pyridine-adsorption (FTIR) was used to estimate Lewis and Bronsted acidities (see **Fig 1**). The measured BET surface areas are also summarized in the table. The XRD patterns of the Y zeolite (**Fig. 2**) are in agreements with those reported in the literature, without the presence of extraneous peaks.

4.2 Disproportionation of Toluene

FCC-Y zeolite was used in the disproportionation reaction of toluene. However, no transformation of toluene into xylenes was observed for this catalyst. This result may be attributed to the low acidity of the Y-zeolite (0.033mmol/g) which is lower than the minimum value required to transform toluene into xylenes. **Table 2** shows the conversions of toluene at different reaction conditions using FCC-Y.

Several more experiments were conducted at both 500 and 450^{o}C to ascertain the results of toluene conversion over FCC-Y catalyst. However, our results still showed that FCC-Y is almost inactive in converting toluene under our experimental conditions. In fact, the new data are quite in agreement with the results in **Table 2**.

However, on a non-steamed Y-zeolite with 0.5 mmol/g acidity, more appreciable toluene conversion was found. It can be concluded then that at FCC conditions toluene is almost non-reactive and higher acidity is needed to help form the activated complex. These findings are in agreement with Xiong[1] who found that toluene conversion is controlled by the concentration of acid sites.

4.3 m-Xylene Transformation Reactions

m-xylene isomerization (I) and disproportionation (D) have been used for characterization of acidic zeolites. *m*-xylene isomerizes to the *para* and *ortho* isomers and can disproportionate into trimethylbenzenes (TMBs) and toluene as illustrated in Scheme 1. Both the isomerization and disproportionation reactions have been reported to be catalyzed by Brönsted acid sites, and disproportionation being a bimolecular reaction has been established to require higher concentration of acid sites [12].

Reaction results of *m*-xylene over FCC-Y at different reaction temperatures and contact times are presented in **Table 3.** Disproportionation of *m*-xylene produces toluene and trimethylbenzenes whereas isomerization gives *o*- and *p*-xylene isomers. Only minor amount of benzene and tetramethylbenzene (TeMB) was found in the reaction products. It is observed from **Table 3**, conversion of *m*-xylene increases with reaction time for all temperatures studied.

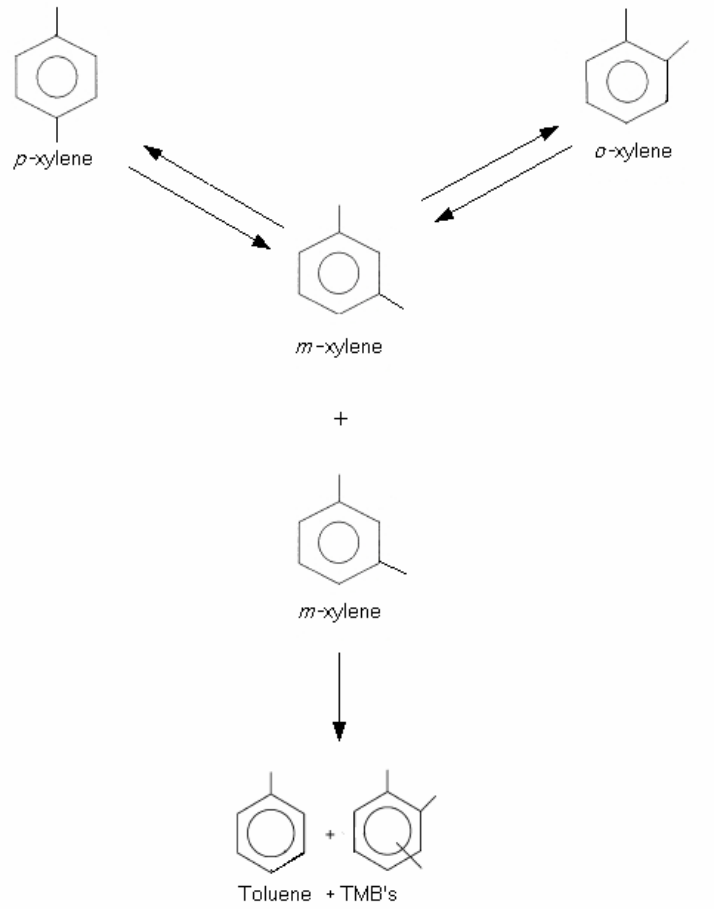

Scheme1

The effect of temperature on *m*-xylene conversion is also reported in **Table 3**. At 15s, the conversion increased from 14.69% at 400^{o}C to 23.37% at 450^{o}C, an increase of about 37.14%. However, the conversion only increased from 23.37% at 450^{o}C to about 29.14% at 500^{o}C, an increase of only about 19.8%. A phenomenon of reduced increases in conversion as the temperature rises exist in the FCC-Y catalyst.

Disproportionation reaction requires two molecules of xylene reactants as bulky bimolecular transition state intermediates. As a result, disproportionation is significant on large pore zeolites that can accommodate these intermediates. **Table 3** shows that initially (at low conversion) isomerization (I) is greater than disproportionation (D) over the FCC-Y zeolite. However, the scenario is reversed as *m*-xylene conversion increases. At 3% conversion and 400^{o}C, the I/D is about 1.5 which decreases to 0.8 at 10% conversion and same temperature. This behavior clearly indicates that as reaction time increases, *m*-xylene is transformed to toluene and trimethylbenzene through the disproportionation reaction.

This secondary transformation appears to be function of reaction time or *m*-xylene conversion. This observation is in agreement with the fact the disproportionation requires higher activation energy than isomerization as reported by Iliyas and Al-Khattaf [16].

Toluene to trimethylbenzene distributions at various conversion levels over the FCC-Y catalyst is shown in **Table 3.** As depicted in this table, T/TMBs ratio is higher than the stoichiometric ratio of 1.0. The higher ratio of T/TMBs could be due to the slow desorption rate of trimethylbenzene isomers [33]. In addition, since TMBs are necessary intermediates for coke formation, conversion of TMBs to coke may also serve as explanation for the low TMB yield in relation to toluene [34,35].

xylene transformation generally gives more 1,3,5-trimethylbenzenes than 1,2,3-trimethylmethylbenzene. The distribution of 1,3,5-to1,2,3-isomer over the FCC-Y catalyst is presented in **Table 3.** The ratio of 1,3,5-to 1,2,3-isomer lies around 3.3 at 400^{o}C, which decreased to 2.35 at 500^{o}C. The ratio is a strong function of temperature and does not seem to change with *m*-xylene conversion.

4.4 1,2,4-Trimethylbenzene Transformation Reactions

The results of transformation reaction of 1,2,4-TMB over FCC-Y at different reaction temperatures and contact times are presented in **Table 4.** The experimental results show that isomerization, disproportionation and transalkylation reactions are taking place. The disproportionation reaction involves the formation of xylenes and tetramethylbenzenes (TeMB) from 2 molecules of 1,2,4-TMB. Subsequently, the xylenes (one of the disproportionation product) react with the TMB to form a transalkylation product toluene as illustrated in scheme 2.

The data from the isomerization reaction show that higher amounts of 1,3,5-TMB were found as compared to the 1,2,3-TMB. Furthermore, three different isomers of tetra methylbenzenes (TeMB) were detected (1,2,4,5-TeMB, 1,2,3,5-TeMB and 1,2,3,4-TeMB). Benzene and pentamethylbenzene (PeMB) have been found to be negligible. Only minor amount of gaseous products was formed, indicating negligible dealkylation in our reaction condition. The experiments also suggest that the distribution of the xylenes and tetra methylbenzenes in the disproportionation products follow closely the values reported in the literature [24, 36, and 37].

Table 4 also shows that conversion of 1,2,4-TMB increases with temperature as well as with reaction time. At 15s, the conversion rose from 31.25% at 400°C to 36% at 450°C and then to 38% at 500°C.

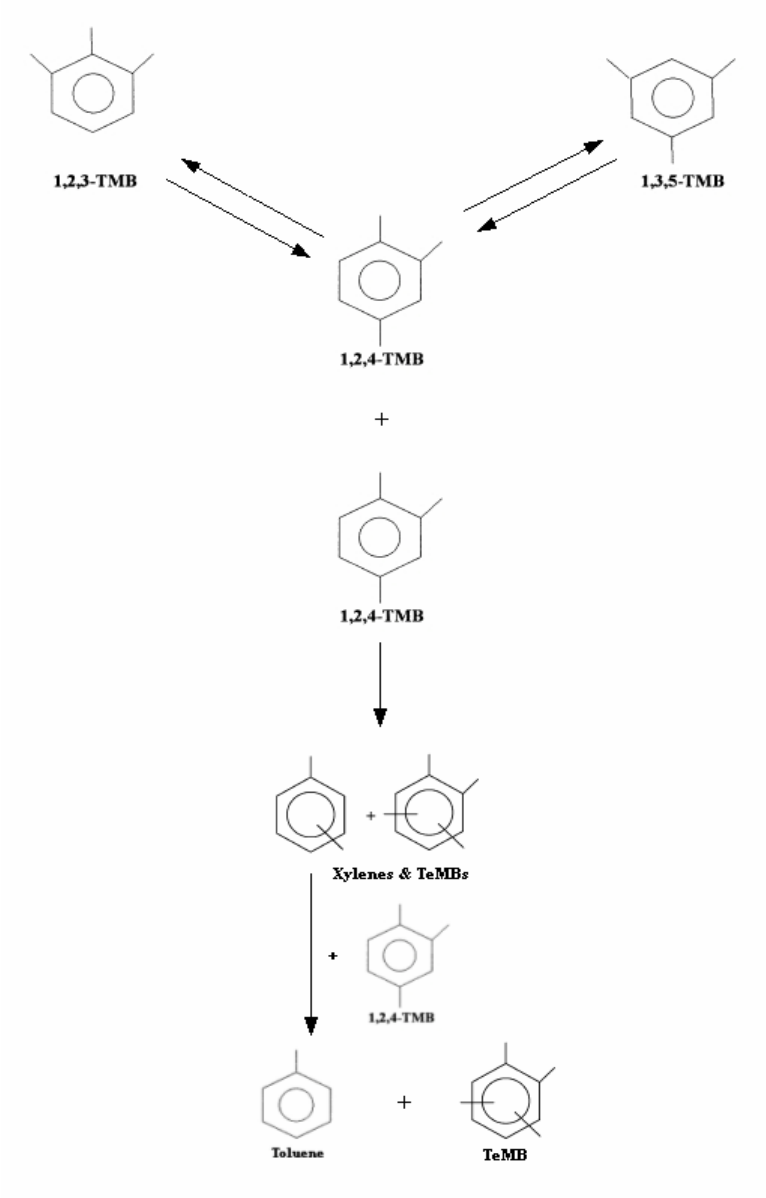

Scheme 2

Unity of xylene-to-tetramethylbenzene (X/TeMB) molar ratio should be obtained if there is no secondary transalkylation or dealkylation [36]. **Table 4** shows xylene-to-tetramethylbenzene (X/TeMB) distributions at various conversion levels over the FCC-Y catalyst. As depicted in this table, X/TeMB ratio is higher than the stoichiometric ratio of 1.0. This is in agreement with the results of Atias et al. [23] who found increased amounts of

xylenes over TeMBs. The higher ratio of X/TeMBs indicates that either secondary transalkylation or dealkylation is taking place. Dealkylation reaction was found to be inconsequential due to the very small amount of gases observed. TeMB may then have been trapped in micropores as coke precursors to account for the excess xylenes in relation to TeMB. This behavior is similar to T/TMB in *m*-xylene conversion. And it can also be attributed to the higher desorption rates of xylenes as compared to tetramethylbenzenes.

1,2,4-TMB can simultaneously undergo isomerization and disproportionation reactions. Again, **Table 4** shows that the isomerization to disproportionation (I/D) ratio lies between 0.3 and 0.4 at all conversion levels over the catalyst. This indicates that 1,2,4-TMB preferentially undergoes disproportionation as compared to isomerization (approx. 3 times greater) over the FCC-Y catalyst.

Experimental results for Isomerization reaction (**Table 4**) show that higher amounts of 1,3,5-TMB were found as compared to the 1,2,3-TMB even though the 1,2,3-isomer has a smaller molecular size than 1,3,5-TMB [38]. However, 1,3,5-TMB is thermodynamically favored over the 1,2,3-isomer [39]. The ratio of 1,3,5- to-1,2,3-isomer over the FCC-Y is about 2.0 and is invariant with conversion but decreases slightly with temperature. Wang et al. [36] reported a value of 2.7 for the1,3,5-/1,2,3-trimethylbenzene ratio at 348^{o}C over USY zeolite. While Park and Rhee [37] reported the ratio 1,3,5-/1,2,3-TMB as 1.99 over HNU-87 (a zeolite with catalytic properties falling between those of medium and large pore zeolites).

4.5 Kinetic Parameters and Model Predictions

The intrinsic kinetic parameters ($k_0^{'}$, E_R & α) for the TOS model were determined for both *m*-xylene and 1,2,4-TMB transformation reactions over the FCC-YZ catalyst using non linear regression of the conversion data. The values of the intrinsic kinetic parameters obtained along with their corresponding 95% confidence limits are presented in **Tables 5 and 7.** The correlation matrixes (**Table 6** for *m*-xylene and **Table 8** for 1,2,4-TMB) displayed low cross-correlation between the regressed parameters showing that the kinetic parameters are accurate.

From the results of the kinetic parameters presented in Table **5**, it is observed that a value of 7.26 kcal/mol was obtained as the activation energy of reaction (E_R) of *m*-xylene over the FCC-Y , while a lower value of 1.69 kcal/mol was obtained for 1,2,4-TMB. Atias

et al., [23] reported an activation energy of 1.60 kcal/mol for the disproportionation of 1,2,4-TMB over large zeolite crystallites (CAT-LC) using Time-on-Stream model. The ease of transformation in the FCC-Y for the 1,2,4-TMB molecule as compared to the *m*-xylene can be attributed to the fact that 1,2,4-TMB with three methyl groups has more opportunity to have contact with active sites that *m*-xylene with only two methyl groups.

Mild diffusional constraints were observed for the 1,2,4-TMB, while no diffusional limitation was seen for the *m*-xylene over the FCC-Y zeolite catalyst. At 400^{o}C and 3s reaction time, an effectiveness factor η_{ss}=0.99 ($h^{'}$*=0.17)* was observed for *m*-xylene and η_{ss}=0.81 ($h^{'}$*=0.86)* for the 1,2,4-TMB as illustrated in. **Fig. 3** where effectiveness factor is plotted against modified Thiele Modulus over all experimental conditions investigated. Effectiveness factor increases with reaction time and temperature, with the tendency to reach close to unity indicating reaction controlled regime (with no diffusional limitations).

Figs. 4 & 5 show comparisons between experimental conversions and model predicted values. As observed in these plots, the model predictions compare favorably with the obtained experimental data for the various conditions. As indicated in **Tables 5 and 7**, the parameters fit the data with regression coefficients of 0.98 and 0.99 for *m*-xylene & 1,2,4-TMB respectively.

4.6 Comparison of the results of transformation reactions of 1,2,4-TMB, m-Xylene and Toluene

4.6.1 Reactivity

Conversions of these reactants are plotted versus reaction time over FCC-Y catalyst in Figures **6a & 6b** at 400^{o}C and 500^{o}C respectively. The plots clearly show that trimethylbenzene is much more reactive than both *m*-xylene and toluene, while *m*-xylene is more reactive than toluene under our present experimental conditions. The much higher reactivity of the trimethylbenzene may be due to the higher number of methyl group attached to its benzene ring which enables it to undergo much deeper reactions than the others.

Furthermore, Cejka et al. [24] measured the diffusion coefficients of 1,2,4-TMB, *m*-xylene and others over known zeolites, and found that the values of the diffusion coefficient were decreasing in the order *m*-xylene >> 1,2,4-TMB. Thus, higher diffusivity does not necessarily point to higher reactivity. The reactivity of these methyl benzene molecules is

clearly shown to be a function of the number of methyl group mainly. For example, toluene has the highest diffusivity and was found the least reactive.

4.6.2 Isomerization versus Disproportionation

The ratio of the rates of isomerization to disproportionation (I/D) is useful for providing information relating to zeolite pore size. Since disproportionation requires a bimolecular reaction, larger pore systems that can accommodate the required transition state give more disproportionation [13]. Plots of isomerization to disproportionation (I/D) ratio are shown in **Figures 7a & 7b** over the FCC-Y catalyst to illustrate the dependence of the (I/D) ratio on the reactant conversions at 500^{o}C.

The results of this study have shown that for *m*-xylene transformation over the FCC-Y catalyst, isomerization is about 1.5-0.8 times greater than disproportionation at 400^{o}C, and only 0.7-0.9 times greater at 500^{o}C. This shows that I/D ratio is a function of temperature and to some extent reaction time for the *m*-xylene transformation. However, isomerization to disproportionation ratio (I/D) for 1,2,4-TMB transformation reactions on the other hand indicates that 1,2,4-TMB preferentially undergoes disproportionation as compared to isomerization in the FCC-Y. Disproportionation was found to be approximately 2.5 times greater than isomerization (I/D ratio = 0.4) at both 400^{o}C and 500^{o}C (**Figs. 7a & 7b**).

4.6.3 p-Xylene to o-Xylene (P/O) ratio

The *p*-Xylene to *o*-Xylene (P/O) ratio provides very good insights as well into the zeolite pore size. Larger values of the P/O ratio point to small pores while lower values tend to show existence of large pores. Generally, P/O ratio increases with both temperature and conversion. This behavior might be due to the increased coke deposition as temperature increases leading to the narrowing of the zeolite channel thereby giving *p*-xylene (kinetic diameter, d_k = 0.58nm) advantage over *o*-xylene (d_k = 0.68nm).

The ratios of *para*- to *ortho*-xylene (P/O) in the product mixture are presented in **Figures 8a & 8b** over the FCC-Y catalyst for *m*-xylene. The P/O ratio averages 0.8 over the whole conversion range at 400^{o}C and 0.9 at 500^{o}C. The P/O ratio over the FCC-Y is well below the equilibrium value of 1.0. Thus, FCC-Y does not show *para*-selectivity during the *m*-xylene transformation.

Similarly, for 1,2,4-TMB transformation, the P/O ratio lies between 0.7 and 0.8 and its change with conversion is very minute. Similar ratios were obtained by Park et al. [37] over HMCM-22 at 350^{o}C. This shows that over FCC-Y, 1,2,4-TMB transformation reaction produces more *o*-xylene than *p*-xylene at all conversion levels, and is therefore not *para*-selective for the 1,2,4-TMB transformation reaction. The mechanism based on biphenyl-methane carbonium ion intermediates [38] has been proposed to explain this phenomenon.

4.6.4 1,3,5-TMB to 1,2,3-TMB ratio

The distribution of trimethylbenzenes can also provide useful insights into the zeolite pore structure. Zeolites with large cages generally should favor the formation of the larger 1,3,5-TMB molecule, while small pore zeolites favor 1,2,3-TMB isomer. However, experimental results for both *m*-xylene and 1,2,4-TMB transformation reactions have shown that higher amounts of 1,3,5-TMB were found as compared to the 1,2,3-TMB.

Figures 9a & 9b depict the relationship between the 1,3,5-TMB/1,2,3-TMB ratio and conversion. For the *m*-xylene transformation reaction, the FCC-Y gave a ratio of about 3.3 at 400^{o}C and 2.4 at 500^{o}C. While the 1,3,5-TMB/1,2,3-TMB ratio of about 2.0 was obtained for the 1,2,4-TMB transformation under the same experimental conditions. This is not far from the thermodynamic equilibrium value of 2.7 reported over USY at 344^{o}C [39].

5. Conclusions

The following conclusions can be drawn from the catalytic transformation of the three methyl benzenes (*toluene, m-xylene, and 1,2,4-trimethyl benzene*) over the USY based FCC-zeolite catalyst in fluidized bed reactor (riser simulator) under the conditions of the experimental study:

1. The reactivity of the methyl benzenes was found to increase in the sequence: *toluene < m-xylene < 1,2,4-trimethyl benzene*. This is attributed to the increase in the number of methyl group attached to the benzene. This is true over the FCC-Y zeolite catalyst for all investigated temperatures.

2. The results show that catalytic activity of methyl benzene molecules transformation is a strong function of the number and position of the methyl group attached to the benzene ring. Diffusion phenomenon is not the only parameter that dominates the transformation reaction as higher diffusivity does not necessarily translate to higher reactivity, as toluene with the highest diffusivity was found the least reactive.

3. Investigation into the various ratios that provide useful insights into the pore structure of zeolite catalysts (I/D, P/O, 1,3,5-TMB/1,2,3-TMB) show that the *m*-xylene transformation produces more isomerization products than disproportionation. While on the other hand, 1,2,4-TMB transformation gave more disproportionation compared to isomerization. Furthermore, the *m*-xylene reaction consistently gave higher P/O & 1,3,5-TMB/1,2,3-TMB ratios than the 1,2,4-TMB reaction over the FCC-Y catalyst.

4. The present results suggest that isomerization reaction favors *p*-xylene formation while disproportionation favors *o*-xylene.

5. The effectiveness factor shows that 1,2,4-TMB transformation has a mild transport restriction in Y-zeolite, in contrast to *m*-xylene transformation that is purely reaction controlled.

Acknowledgement

This project is supported by the King AbdulAziz City for Science & Technology (KCAST) under project # AR-22-14. Also the support of King Fahd University of Petroleum & Minerals is highly appreciated.

Nomenclature

C_A	reactant concentration in the riser simulator (mole/m^3)
CFL	confidence limit
E_R	energy of activation due to reaction, kcal/mol
E_D	energy of activation due to diffusion, kcal/mol
$k_{A,in}$	Intrinsic kinetic rate constant (m^3/kgcat.sec)
	$= k'_0 exp[\frac{-E_R}{R}(\frac{1}{T}-\frac{1}{T_0})$
$k_o^{'}$	Pre-exponential factor in Arrhenius equation defined at an average temperature [m^3/kgcat.sec], units based on first order reaction
D_o	Diffusion coefficient constant, m^2/s
D_{eff}	Effective Diffusion coefficient, m^2/s
$h^{'}$	$\frac{1}{a_{ext}}\sqrt{\frac{k_{A,in}\rho_{cr}\varphi_{in}}{D_{eff}}}$; Modified Thiele Modulus
η_{ss}	$\frac{\tanh(h^{'})}{h^{'}}$; Effectiveness factor
ρ_{cr}	Density of zeolite crystal, kg/m^3
r	correlation coefficient
R	universal gas constant, kcal/kmol K
t	reaction time (sec).
T	reaction temperature, K
To	average temperature of the experiment, K
V	volume of the riser (45 cm^3)
W_{cr}	mass of the catalysts (0.81 gcat)
y_A	reactant mass fraction (wt%)

Greek letters

α	apparent deactivation constant, s^{-1} (TOS Model)
φ	apparent deactivation function, dimensionless

Literature Cited

1. Xiong, Y., Rodewald, P. G., and Chang, C. D. *J. Am. Chem. Soc*. **1995**, 117, 9427.

2. Kim, J. H., Namba, S., and Yashima T. *Appl. Catal*. A **1992**, 83, 51.

3. Kurschner, U., Jerschkewitz, H. G., Schreier, E., and Volter, J. *Appl. Catal*. **1990**, 57, 167.

4. Tsai, T.C, Liu, S.B, and Wang, I, *Appl. Catal. A*: *General* **1999**, 181, 355-398.

5. Chen, N. Y., Kaeding, W. W., and Dwyer, F. G. *J. Am. Chem. Soc.* **1979**, 101, 6783.

6. Olson, D. H., and Haag, W. O. ACS Syp. Ser. 1984, 248, 275.

7. Cejka, J., and Wichterlova, B. *Catal. Rev*. **2002**, 44, 375-421.

8. Morin, S.; Gnep, N. S.; Guisnet, M. *J. of Catal.* **1996**, 159(2), 296-304.

9. Morin, S.; Ayrault, P.; Gnep, N.S.; Guisnet, M. *Appl. Catal. A: General* **1998**, 166(2), 281-292.

10. Corma, A.; Sastre, E. *J. Catal*. **1991**, *129*, 177.

11. Corma, A.; Sastre, E. Chemical Communications **1991**,(8), 594.

12. Vinek, H., and Lercher, J. A. *J. Mol. Catal*. **1991**, 64, 23.

13. Jones, C. W., Zones, S. T., and davis, M. E. *Appl. Catal*. **1999**, 181, 289-303.

14. Martens, J. A., Perez-Pariente, J. Sastre, E., Corma, A., and Jacobs, P. A. *Appl. Catal*. A **1988**, 45, 85-101.

15. Adair, B., Chen, C. Y., Wan, K. T., and Davis, M. E. *Microporous Mater*. **1996**, 7, 261-270.

16. Iliyas, A., and Al-Khattaf, S. *Ind. Eng. Chem. Res.,* **2004**, 43, 1349.

17. Iliyas, A., and Al-Khattaf, S. *Appl. Catal. A: Gen,* **2004**, 269, 225.

18. Al-Khattaf, S., N. M. Tukur., and A. Al-Amer. *Ind. Eng. Chem. Res.,* **2005,** 44, 7957.

19. Collins, D. J., Quirey, C. B., Fertig, J. E. and Davis, B. *Appl. Catal.* **1986**, 28**,** 35-55.

20. Matsuda .T, Asanuma, M., and Kikuch1, E., *Appl. Catal. A: General* **1988**, 38, 289-299.

21. Roger, H. P., Moller, K. P. and O'Connor, C. T. . *J. Catal*. **1998**, 176, 68-75.

22. Roger, H. P., Bohringer, W., Moller, K. P. and O'Connor, C. T. *Studies in Surf. Sci. and Catal.* **2000**, 130**,** 281-286.

23. Atias, J. A., Tonetto, G. and de Lasa, H. *Ind. Eng. Chem. Res.* **2003**, 42, 4162-4173.

24. Cejka, J., Kotrla, J. and Krejci, A. *Appl. Catal.* A: General **2004**, 277, 191-199.

25. de Lasa, H. T., US Patent 5 **1992**, 102, 628.

26. Al-Khattaf, S, and de Lasa, H. I. *Ind. Eng. Chem. Res.* **2001**, 40, 5398.

27. Al-Khattaf, S, and de Lasa, H. I. *Chem. Eng. Sc.* **2002**, 57, 4909.

28. Al-Khattaf, S, and de Lasa, H. I. *Appl. Catal. A: Gen,* **2002**, 226, 139.

29. Al-Khattaf, S. *Appl. Catal. A: Gen,* **2002**, 231, 293.

30. Kraemer, D. W., Ph.D. Dissertation, University of Western Ont., London, Canada **1991**.

31. Voorhies, A. Jr., Ind. Eng. Chem., **1945**, 37, 318.

32. Germanus, A., Karger, J., Pfeifer, H., Samulevic, N. N. and Zhdanov, S. P. *Zeolites* **1985**, 5, 91.

33. Gnep, N.S, and Guisnet, M, , *Appl. Catal. A: General* **1981**, 1, 329.

34. Laforge, S., Martin, D., Paillaud, J. L., and Guisnet, M. *J. Cat*., **2003**, 220, 92.

35. Nakazaki, Y., Goto, N., and Inui, T. *J. Cat*. **1992**, 136, 141.

36. Wang, I., Tsai, T-C, and Huang, S-T. *Ind. Eng. Chem. Res.* **1990**, 36, 1812.

37. Park, S-H, Rhee, H-K. *Catalysis Today*, **2000**, 63, 267.

38. Csicsery, S. M. *J. Catal,* **1971**, 23, 124

39. Earhart, H. W. Polymethylbenzenes. *Kirk-Othmer Encyclopedia of Chemical technology*; Wiley: New York, **1982**, Vol. 18, p 882.

List of Tables

Table 1: Characterization of used Catalyst

Catalyst	Acidity (mmol/g)	Lewis sites %	Bron sites %	Surface Area (m^2/g)	Crystall-ite size (μm)	Unit cell size (Å)	SiO_2/Al_2O_3 (mol/mol)	Na_2O wt %
FCC-Y	0.033	65	35	197	0.9	24.27	5.7	Negligible

Table 2: Toluene conversions (%) at different reaction conditions over FCC-Y

Temp (^oC)/ time (s)	Conversion (%)
350	
5	0.26
10	0.353
400	
5	0.39
10	0.517
450	
5	0.56
10	0.84
500	
5	0.89
10	1.65

Table 3: Product distribution (wt %) at various reaction conditions for *m*-xylene transformation over FCC-Y

Temp (^oC)/ time (s)	Conv. (%)	Gas	Benzene	*m*-xylene	*p*-xylene	*o*-xylene	**TI***	Toluene	*1,3,5* TMB	*1,2,4* TMB	*1,2,3* TMB	TeMB's	**TD****
400													
3	3.80	-	-	96.21	0.96	1.29	2.25	0.81	0.17	0.41	0.05	-	1.44
5	6.59	-	-	93.41	1.57	1.86	3.43	1.64	0.38	0.92	0.13	-	3.07
7	7.022	-	-	92.98	1.67	1.95	3.62	1.73	0.43	1.03	0.15	-	3.34
10	9.6	-	-	90.42	1.99	2.35	4.34	2.59	0.69	1.62	0.20	0.05	5.10
15	14.69	-	0.06	85.31	3.26	3.49	6.75	3.78	1.03	2.50	0.33	0.17	7.64
450													
3	6.94	-	0.05	93.06	1.57	1.89	3.46	1.77	0.38	1.00	0.14	0.05	3.29
5	9.26	-	0.08	89.75	2.23	2.51	4.74	2.71	0.63	1.62	0.24	0.15	5.20
7	12.6	-	0.11	87.41	2.64	2.93	5.57	3.39	0.82	2.11	0.31	0.21	6.63
10	17.7	-	0.15	82.31	3.66	3.90	7.56	4.78	1.20	3.09	0.46	0.38	9.53
15	23.37	-	0.18	76.63	4.92	5.07	9.99	6.26	1.61	4.14	0.63	0.51	12.64
500													
3	8.02	-	0.11	91.98	1.67	2.01	3.68	2.12	0.46	1.24	0.19	0.15	4.01
5	12.11	-	0.18	87.88	2.42	2.72	5.14	3.33	0.76	2.04	0.33	0.27	6.46
7	15.6	-	0.23	84.44	3.03	3.31	6.34	4.32	1.02	2.73	0.43	0.42	8.50
10	21.30	-	0.29	78.70	4.13	4.35	8.48	5.93	1.44	3.87	0.61	0.61	11.85
15	29.14	0.07	0.40	70.87	5.59	5.77	11.36	8.14	2.01	5.37	0.87	0.87	16.39

*TI – Total isomerization

**TD – Total Disproportionation

Table 4: Product distribution (wt %) at various reaction conditions for *1,2,4-Trimethylbenzene* transformation over FCC-Y

Temp (^{o}C)/ time (s)	Conv. (%)	Gas	Benzene	*1,3,5*-TMB	*1,2,3*-TMB	**TI***	*p*-xylene	*m*-xylene	*o*-xylene	Toluene	TeMB's (1,2,3,4-, 1,2,3,5-, & 1,2,4,5)	**TD****
400												
3	8.12	-	-	1.33	0.65	1.99	0.55	1.31	0.82	0.30	2.09	5.07
5	12.64	-	-	2.04	0.99	3.03	0.89	2.10	1.30	0.47	3.73	8.49
7	17.40	-	-	2.76	1.34	4.10	1.23	2.89	1.78	0.64	5.48	12.02
10	23.00	0.06	-	3.80	1.84	5.64	1.68	3.98	2.47	0.84	7.99	16.96
13	27.80	0.09	-	4.72	2.27	6.99	2.08	4.92	3.03	1.03	10.22	21.28
15	31.25	0.11	0.04	5.22	2.5	7.72	2.32	5.48	3.37	1.15	11.55	23.87
450												
3	9.90	-	-	1.67	0.82	2.49	0.67	1.54	0.94	0.38	2.75	6.28
5	15.64	0.07	-	2.60	1.26	3.86	1.07	2.48	1.49	0.60	4.80	10.44
7	20.00	0.10	-	3.31	1.60	4.91	1.38	3.19	1.90	0.77	6.42	13.66
10	26.88	0.14	-	4.44	2.12	6.56	1.88	4.33	2.55	1.04	8.97	18.77
13	31.40	0.16	0.05	5.31	2.53	7.84	2.25	5.21	3.06	1.23	11.01	22.76
15	36.0	0.20	0.06	6	2.80	8.8	2.46	5.8	3.37	1.35	12.20	25.09
500												
3	11.48	0.09	-	1.96	0.97	2.93	0.78	1.76	1.02	0.49	3.25	7.30
5	16.22	0.15	-	2.74	1.34	4.08	1.13	2.55	1.46	0.71	4.90	10.75
7	21.44	0.21	-	3.61	1.76	5.37	1.50	3.39	1.94	0.92	6.72	14.47
10	28.20	0.33	0.05	4.73	2.29	7.02	1.98	4.50	2.56	1.23	9.06	19.33
13	34.5	0.34	0.06	5.8	2.7	8.5	2.4	5.6	3.2	1.45	10.80	22.49
15	38.0	0.47	0.07	6.2	2.9	9.1	2.7	6.3	3.5	1.7	11.8	24.70

*TI – Total isomerization

**TD – Total Disproportionation

Table 5: Kinetic constants for *m*-xylene transformation over FCC-Y Based on Time on Stream (TOS Model)

Catalyst	$k_0^{'}$ (m^3/kg-cat.sec)	95% CFL	E_R (kcal/mol)	95% CFL	α (1/sec)	95% CFL	r^2
FCC-Y	1.43E-03	0.24E-03	7.26	1.48	0.051	0.032	0.98

Table 6: Correlation matrix for FCC-Y (*m*-xylene) – TOS Model

$k_0^{'}$	1	-0.16	0.94
E_R	-0.16	1	-0.03
α	0.94	-0.03	1

Table 7: Kinetic constants for 1,2,4-TMB over FCC-Y Based on Time on Stream (TOS Model)

Catalyst	$k_0^{'}$ (m^3/kg-cat.sec)	95% CFL	E_R (kcal/mol)	95% CFL	α (1/sec)	95% CFL	r^2
FCC-Y	2.83E-03	0.24E-03	1.69	0.63	0.046	0.015	0.99

Table 8: Correlation matrix for FCC-Y (1,2,4-TMB) – TOS Model

$k_0^{'}$	1	-0.06	0.96
E_R	-0.06	1	-0.03
α	0.96	-0.03	1

Figure Captions

Figure 1: FTIR spectra of adsorbed pyridine on FCC-Y catalyst

Figure 2: X-ray Diffraction for the USY Zeolite Catalysts used in the study

Figure 3: Effectiveness factor versus modified Thiele Modulus (TOS model). T = 400-500^{o}C, (□) m-xylene, (Δ) 1,2,4-TMB.

Figure 4: Modeling *m*-xylene conversion over FCC-Y. Decay function based on time on stream (TOS)

Figure 5: Modeling 1,2,4-TMB conversion over FCC-Y. Decay function based on time on stream (TOS)

Figure 6: Reactivity comparisons between 1,2,4-TMB transformation (♦), *m*-xylene (□) and toluene (Δ) over FCC-Y at **a)** 400^{o}C; **b)** 500^{o}C

Figure 7: I/D ratio comparisons between 1,2,4-TMB transformation (♦) and *m*-xylene (□) over FCC-Y **a)** at 400^{o}C; **b)** at 500^{o}C

Figure 8: P/O ratio comparisons between 1,2,4-TMB transformation (♦) and *m*-xylene (□) over FCC-Y **a)** at 400^{o}C; **b)** at 500^{o}C

Figure 9: 1,3,5-TMB/1,2,3-TMB ratio comparisons between 1,2,4-TMB transformation (♦) and *m*-xylene (□)over FCC-Y **a)** at 400^{o}C; **b)** at 500^{o}C

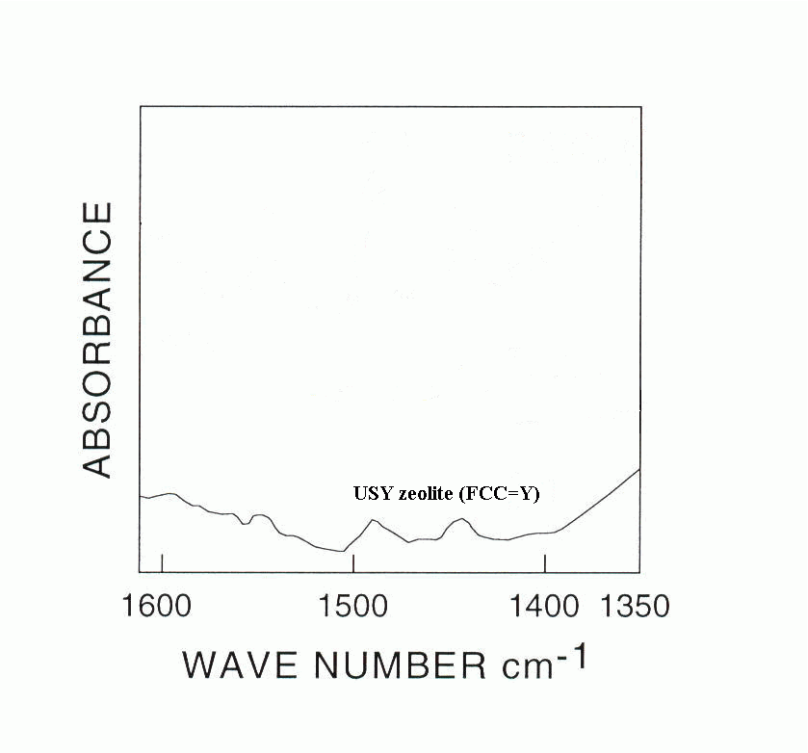

Figure 1: FTIR spectra of adsorbed pyridine on FCC-Y catalyst

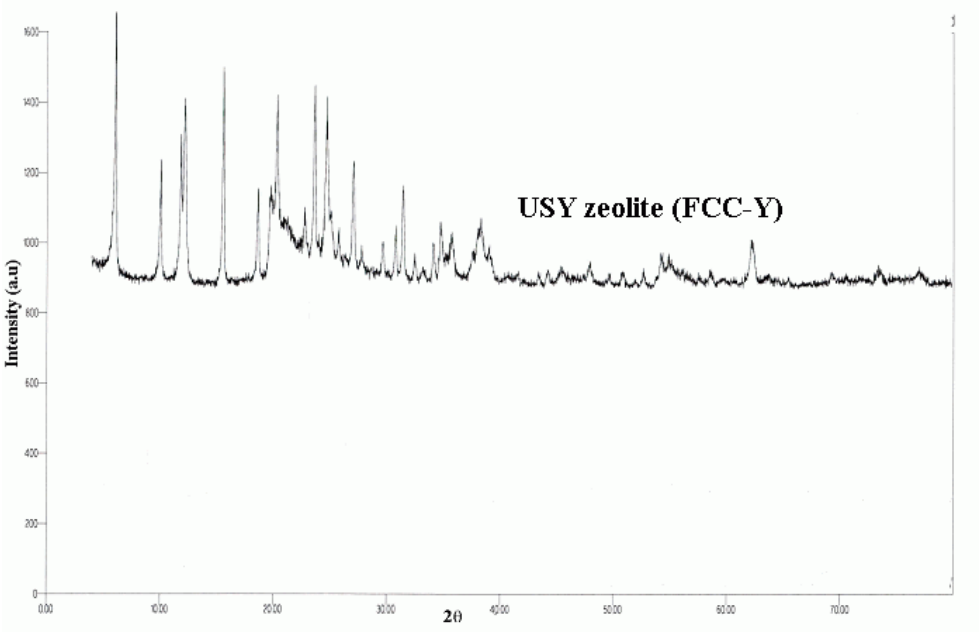

Figure 2: X-ray Diffraction for the USY zeolite catalyst used in the study

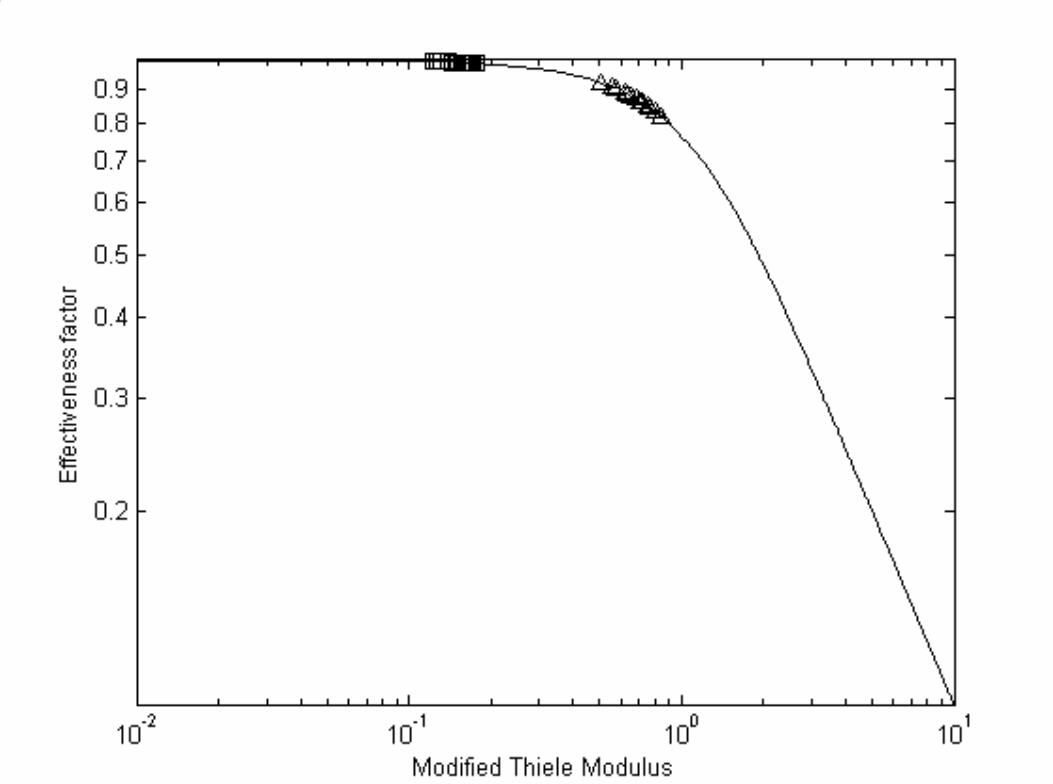

Figure 3: Effectiveness factor versus modified Thiele Modulus (TOS model). T = 400-500^{o}C, (□) m-xylene, (Δ) 1,2,4-TMB.

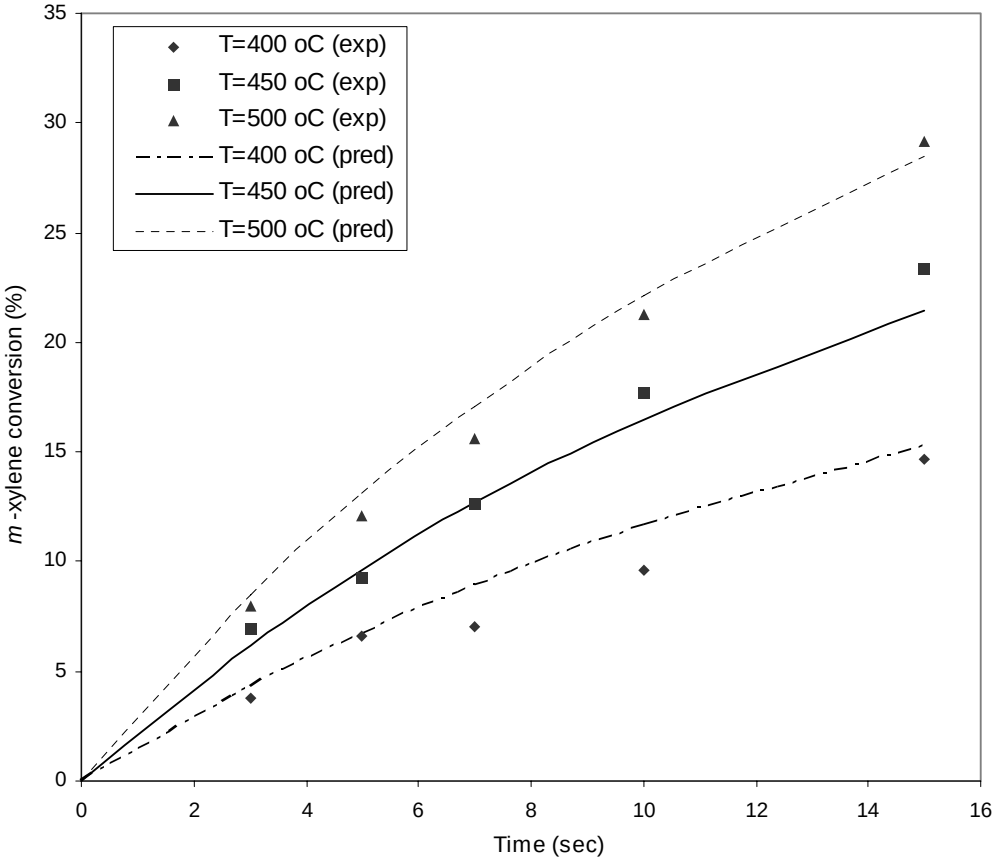

Figure 4: Modeling *m*-xylene conversion over FCC-Y. Decay function based on time on stream (TOS)

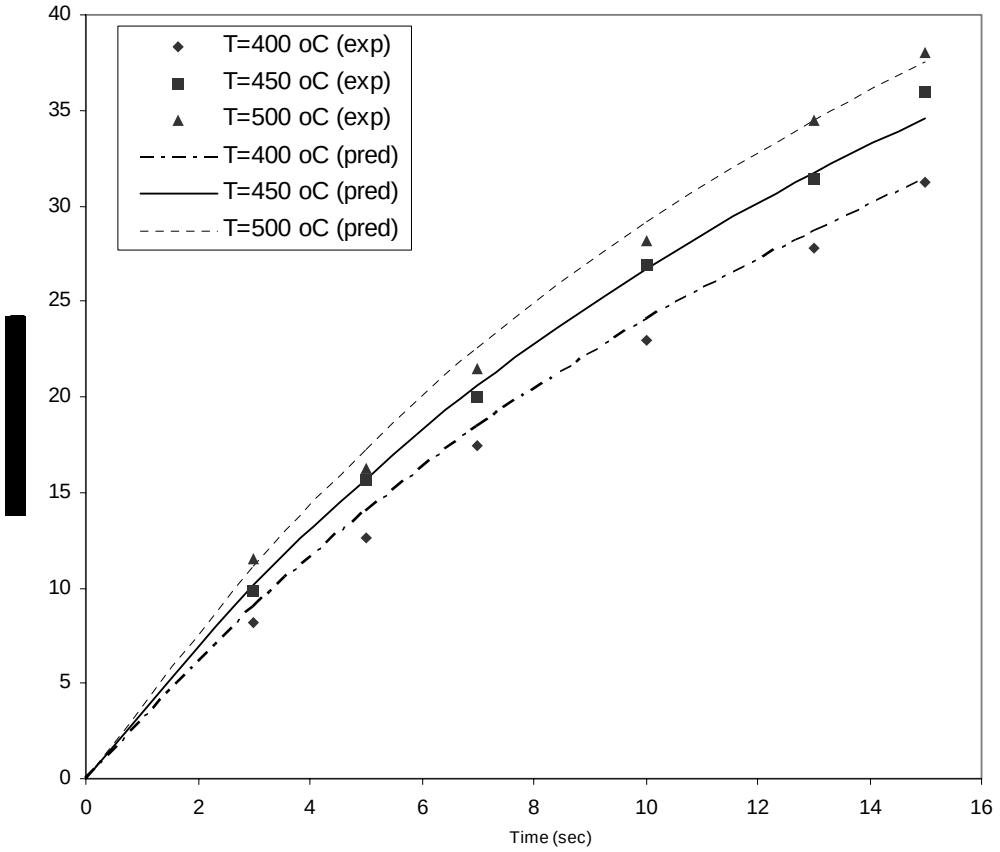

Figure 5: Modeling 1,2,4-TMB conversion over FCC-Y. Decay function based on time on stream (TOS)

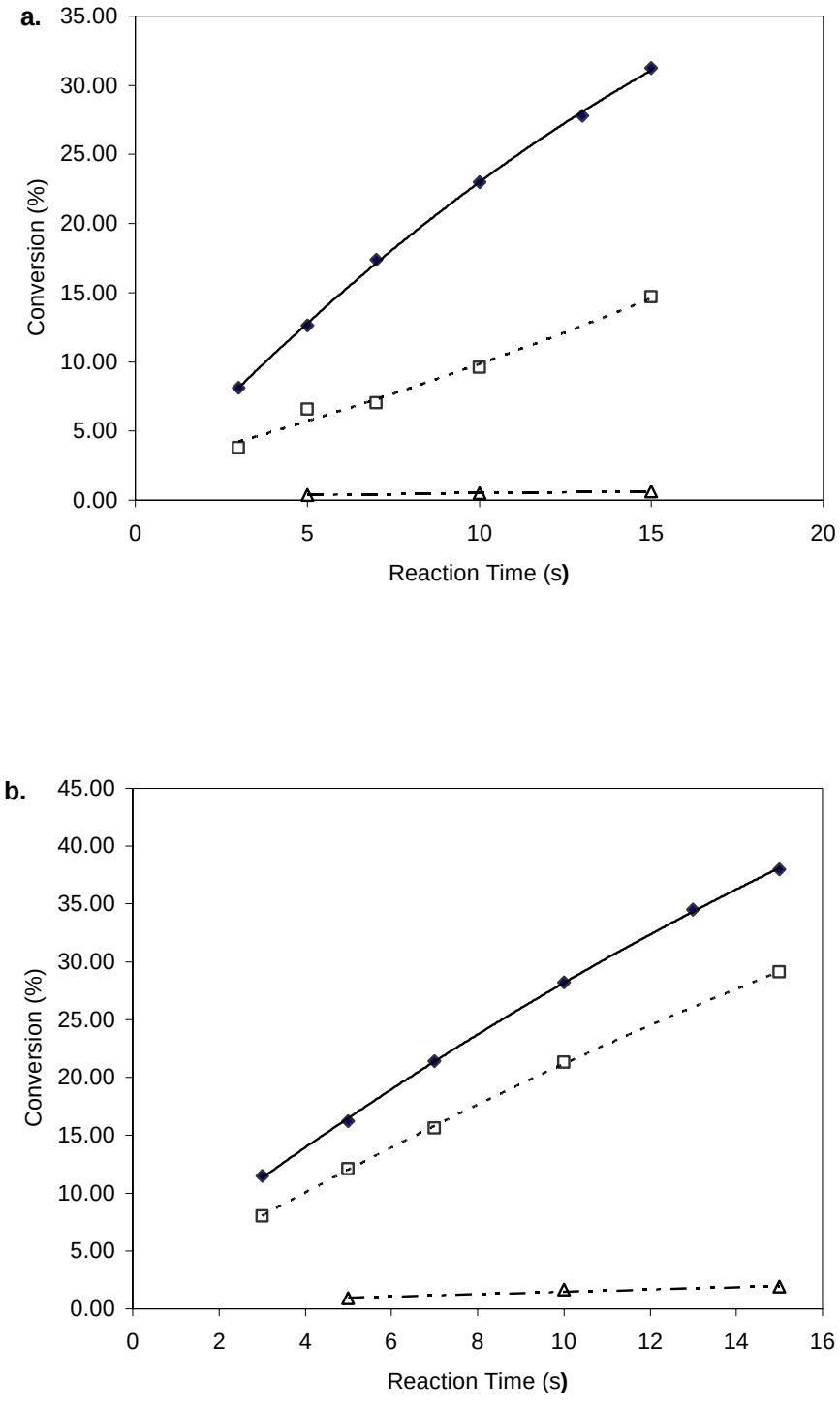

Figure 6: Reactivity comparisons between 1,2,4-TMB transformation (♦), *m*-xylene (□) and toluene (Δ) over FCC-Y at **a)** 400°C; **b)** 500°C

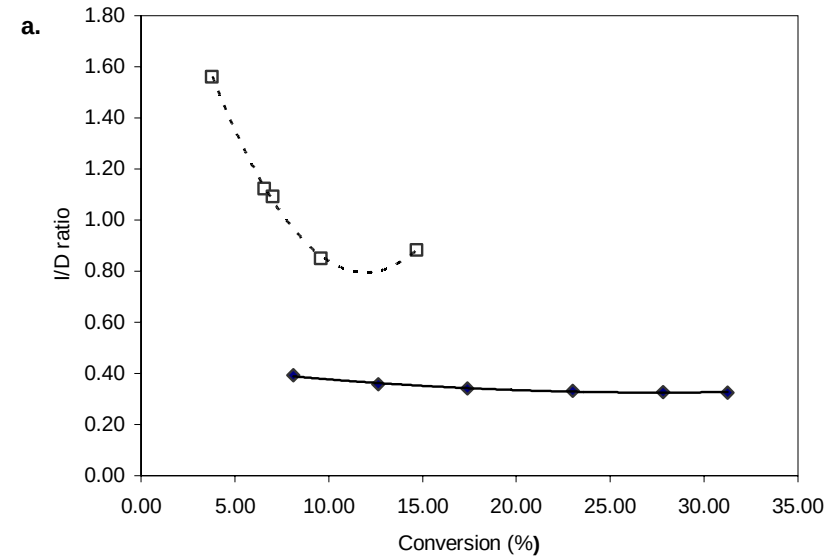

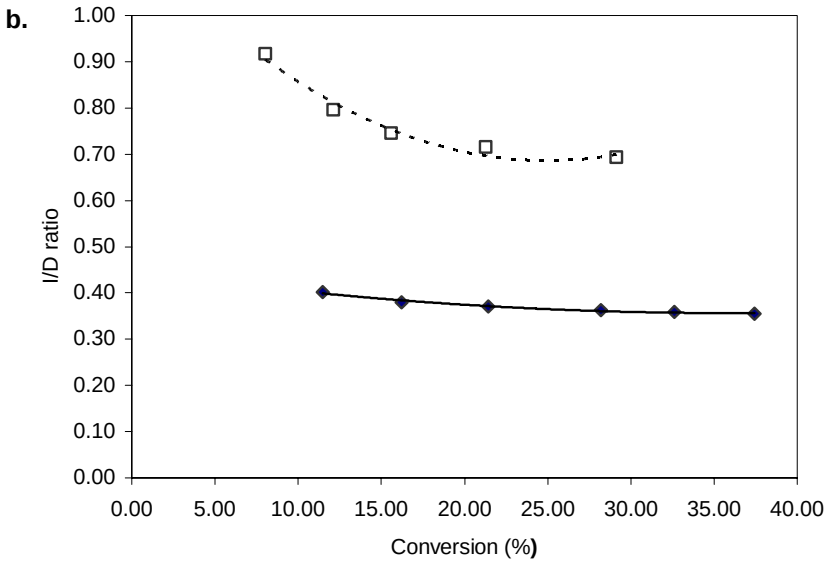

Figure 7: I/D ratio comparisons between 1,2,4-TMB transformation (♦) and *m*-xylene (□) over FCC-Y **a)** at 400°C; **b)** at 500°C

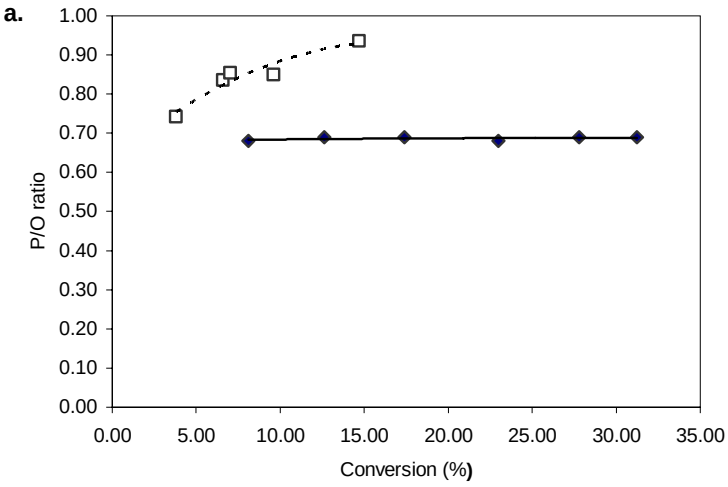

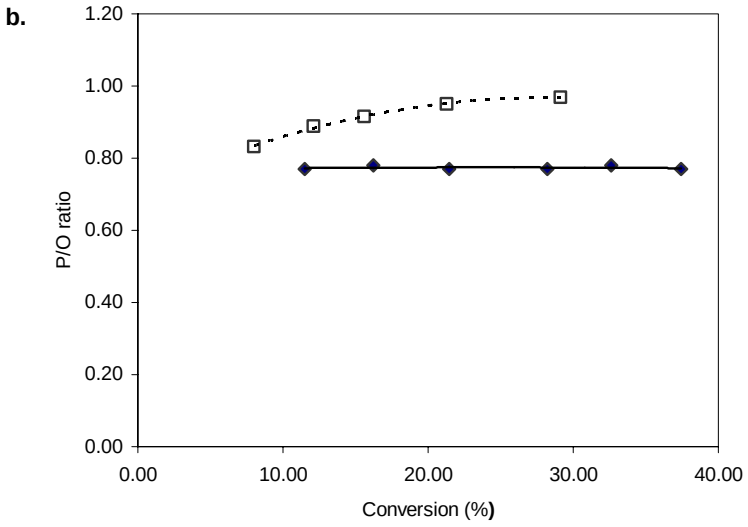

Figure 8: P/O ratio comparisons between 1,2,4-TMB transformation (♦) and *m*-xylene (□) over FCC-Y **a)** at 400°C; **b)** at 500°C

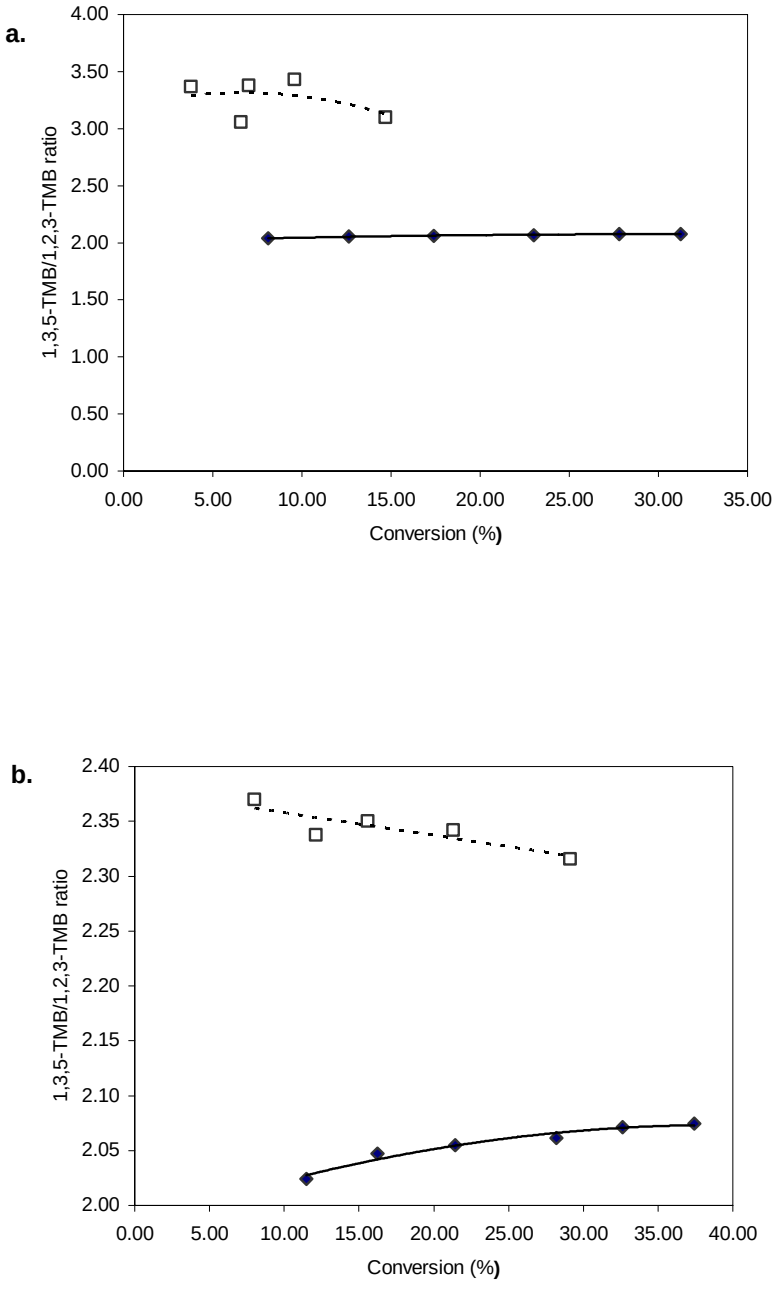

Figure 9: 1,3,5-TMB/1,2,3-TMB ratio comparisons between 1,2,4-TMB transformation (♦) and *m*-xylene (□)over FCC-Y **a)** at 400°C; **b)** at 500°C